Biomedical Optics EXPRESS

Design of miniaturized illumination for transvaginal co-registered photoacoustic and ultrasound imaging

Hassan S. Salehi,[1] Tianheng Wang,[1] Patrick D. Kumavor,[2] Hai Li,[1] and Quing Zhu[1,2,*]

[1]*Department of Electrical and Computer Engineering, University of Connecticut, Storrs, CT 06269, USA*
[2]*Department of Biomedical Engineering, University of Connecticut, Storrs, CT 06269, USA*
[*]*zhu@engr.uconn.edu*

Abstract: A novel lens-array based illumination design for a compact co-registered photoacoustic/ultrasound transvaginal probe has been demonstrated. The lens array consists of four cylindrical lenses that couple the laser beams into four 1-mm-core multi-mode optical fibers with optical coupling efficiency of ~87%. The feasibility of our lens array was investigated by simulating the lenses and laser beam profiles using Zemax. The laser fluence on the tissue surface was experimentally measured and was below the American National Standards Institute (ANSI) safety limit. Spatial distribution of hemoglobin oxygen saturation (sO_2) of a mouse tumor was obtained *in vivo* using photoacoustic measurements at multiple wavelengths. Furthermore, benign and malignant ovaries were imaged *ex vivo* and evaluated histologically. The co-registered images clearly showed different patterns of blood vasculature. These results highlight the clinical potential of our system for noninvasive photoacoustic and ultrasound imaging of ovarian tissue and cancer detection and diagnosis.

OCIS codes: (110.0110) Imaging systems; (170.2945) Illumination design; (170.5120) Photoacoustic imaging; (170.6960) Tomography; (170.7170) Ultrasound.

References and links

1. D. L. Clarke-Pearson, "Clinical practice. screening for ovarian cancer," N. Engl. J. Med. **361**(2), 170–177 (2009).
2. D. A. Fishman, L. Cohen, S. V. Blank, L. Shulman, D. Singh, K. Bozorgi, R. Tamura, I. Timor-Tritsch, and P. E. Schwartz, "The role of ultrasound evaluation in the detection of early-stage epithelial ovarian cancer," Am. J. Obstet. Gynecol. **192**(4), 1214–1221 (2005).
3. M. A. Brewer, U. Utzinger, J. K. Barton, J. B. Hoying, N. D. Kirkpatrick, W. R. Brands, J. R. Davis, K. Hunt, S. J. Stevens, and A. F. Gmitro, "Imaging of the ovary," Technol. Cancer Res. Treat. **3**(6), 617–627 (2004).
4. L. V. Wang and S. Hu, "Photoacoustic tomography: in vivo imaging from organelles to organs," Science **335**(6075), 1458–1462 (2012).
5. S. A. Ermilov, T. Khamapirad, A. Conjusteau, M. H. Leonard, R. Lacewell, K. Mehta, T. Miller, and A. A. Oraevsky, "Laser optoacoustic imaging system for detection of breast cancer," J. Biomed. Opt. **14**(2), 024007 (2009).
6. S. Sethuraman, J. H. Amirian, S. H. Litovsky, R. W. Smalling, and S. Y. Emelianov, "Spectroscopic intravascular photoacoustic imaging to differentiate atherosclerotic plaques," Opt. Express **16**(5), 3362–3367 (2008).
7. X. Wang, Y. Pang, G. Ku, X. Xie, G. Stoica, and L. V. Wang, "Noninvasive laser-induced photoacoustic tomography for structural and functional in vivo imaging of the brain," Nat. Biotechnol. **21**(7), 803–806 (2003).
8. A. Aguirre, Y. Ardeshirpour, M. M. Sanders, M. Brewer, and Q. Zhu, "Potential Role of Coregistered Photoacoustic and Ultrasound Imaging in Ovarian Cancer Detection and Characterization," Trans. Oncol. **4**(1), 29–37 (2011).
9. A. Karabutov, E. V. Savateeva, N. B. Podymova, and A. A. Oraevsky, "Backward mode detection of laser-induced wide-band ultrasonic transients with optoacoustic transducer," J. Appl. Phys. **87**(4), 2003–2014 (2000).
10. J. Gamelin, A. Aguirre, A. Maurudis, F. Huang, D. Castillo, L. V. Wang, and Q. Zhu, "Curved array photoacoustic tomographic system for small animal imaging," J. Biomed. Opt. **13**(2), 024007 (2008).
11. R. A. Kruger, W. L. Kiser, Jr., D. R. Reinecke, and G. A. Kruger, "Thermoacoustic computed tomography using a conventional linear transducer array," Med. Phys. **30**(5), 856–860 (2003).
12. J. Laufer, P. Johnson, E. Zhang, B. Treeby, B. Cox, B. Pedley, and P. Beard, "In vivo preclinical photoacoustic imaging of tumor vasculature development and therapy," J. Biomed. Opt. **17**(5), 056016 (2012).

#213817 - $15.00 USD Received 16 Jun 2014; revised 29 Jul 2014; accepted 11 Aug 2014; published 19 Aug 2014

13. T. Wang, P. D. Kumavor, and Q. Zhu, "Application of laser pulse stretching scheme for efficiently delivering laser energy in photoacoustic imaging," J. Biomed. Opt. **17**(6), 061218 (2012).
14. G. Ku, X. Wang, G. Stoica, and L. V. Wang, "Multiple-bandwidth photoacoustic tomography," Phys. Med. Biol. **49**(7), 1329–1338 (2004).
15. P. D. Kumavor, U. Alqasemi, B. Tavakoli, H. Li, Y. Yang, X. Sun, E. Warych, and Q. Zhu, "Co-registered pulse-echo/photoacoustic transvaginal probe for real time imaging of ovarian tissue," J. Biophotonics **6**(6-7), 475–484 (2013).
16. U. Alqasemi, H. Li, A. Aguirre, and Q. Zhu, "FPGA-based reconfigurable processor for ultrafast interlaced ultrasound and photoacoustic imaging," IEEE Trans. Ultrason., Ferr. Freq. Control **59**(7), 1344–1353 (2012).
17. U. Alqasemi, H. Li, G. Yuan, P. D. Kumavor, S. Zanganeh, and Q. Zhu, "Real-time interlaced ultrasound and photoacoustic system for in vivo ovarian tissue imaging," J. Biomed. Opt. in press.
18. H. S. Salehi, P. D. Kumavor, U. Alqasemi, H. Li, T. Wang, and Q. Zhu, "High-throughput fiber-array transvaginal ultrasound/photoacoustic probe for ovarian cancer imaging," Proc. SPIE **8943**, 894335 (2014).
19. American National Standard for the Safe Use of Lasers, ANSI Z136 (Laser Institute of America, Orlando, Florida, 2007), pp. 1–2007.

1. Introduction

Most ovarian cancers are detected when the cancer has already metastasized to the peritoneum and other organs because there is no adequate technology to detect early stage ovarian cancers. Thus, ovarian cancer has the highest mortality rate of all gynecologic cancers with a 5-year survival rate of approximately 33% when the disease is diagnosed at stage III or IV [1–3]. Therefore, it is significant to improve the current diagnostic techniques and consequently increase the survival rate in patients.

Photoacoustic tomography (PAT) is a hybrid imaging technique that has broad preclinical and clinical applications [4–8]. In PAT, a short laser pulse propagates into a tissue sample diffusively and the photoacoustic signals arising from tissue thermoelastic expansion caused by the laser irradiation are measured around the sample by wideband ultrasound (US) transducers [9–13]. The acquired photoacoustic signals are utilized to reconstruct, at ultrasound resolution, the optical absorption distribution that reveals optical contrast of the tissue. For *in vivo* imaging, the optical absorption of hemoglobin molecules is wavelength dependent. Thus, PAT reveals rich spectroscopic information of tissue vasculature and oxygen saturation (sO_2) when it is illuminated at multiple wavelengths [14]. Monitoring tumor vasculature and oxygenation is clinically important because abnormal vascularization and lower blood oxygenation in tumors could indicate the presence of malignant carcinomas.

We have developed a co-registered photoacoustic/ultrasound system and probe for noninvasive transvaginal examination of the ovaries [15–18]. In our previous study [18], we designed a photoacoustic/ultrasound transvaginal probe with optimized light delivery using four optical fibers. However, the optical setup was bulky and complicated. In order to split the original laser beam and couple the light into those four fibers, three beamsplitters, two mirrors, and four focal lenses were implemented. In fact, all those optical components could be replaced with one homemade lens array to achieve the same objective. In this paper, we report a novel compact design, implementation, and evaluation of a light illumination setup for real-time imaging of ovarian tissue using co-registered photoacoustic/ultrasound transvaginal probe that is suitable for clinical studies at operating rooms. The light delivery system consists of a single homemade lens array, a custom-made transducer sheath lined with highly reflecting aluminum material, and four 1-mm-core multi-mode optical fibers surrounding the ultrasound transducer to illuminate the tumor region efficiently. The laser output energy and laser energy density of the probe were experimentally measured, which were below the ANSI safety limit. By utilizing photoacoustic measurements at multiple wavelengths, hemoglobin oxygen saturation (sO_2) of a mouse tumor was noninvasively imaged *in vivo*. In another set of experiments, human ovaries were imaged *ex vivo*. These results demonstrate the clinical potential of our system in identifying vasculature and blood oxygenation in tumors.

#213817 - $15.00 USD Received 16 Jun 2014; revised 29 Jul 2014; accepted 11 Aug 2014; published 19 Aug 2014

2. Methods and materials

2.1 Simulation of illumination design

The lens array design was first performed by simulating four cylindrical lenses in Zemax. In order to split a laser beam into four spots, two cylindrical lenses were vertically placed in front and the other two horizontally arranged behind (rotated 90°) with respect to the front lenses, as shown in Fig. 1(a). The laser light was simulated as Gaussian light source with optical wavelength of 750nm. The laser beam profiles were obtained at different distances from the lens array to find the optimal distance for coupling the light into optical fibers.

2.2 Photoacoustic/ultrasound imaging system

In the experimental setup of the PAT imaging, the laser light propagates through the single homemade lens array that consists of four cylinder lenses (12.5mm H x 25mm L x 150mm FL Cylinder Lens VIS-NIR Coating, Edmund Optics PCX). The lens array splits the incoming incident light into four beams. Each beam is then directed to couple into a 1mm-core optical fiber with a numerical aperture (NA) of 0.48. The optical coupling efficiency is determined from the ratio of the measured total energy output from the four fibers to the total energy incident at their input end faces, and is ~87%. The optical fibers are mounted on a single adjustable platform as shown in Fig. 1(a). The illumination fibers are then affixed to a compact photoacoustic/ultrasound imaging probe. The probe consists of a 128-element transvaginal ultrasound transducer array of 6MHz central frequency and 80% bandwidth (W.L. Gore and Associates, Inc., Newark, DE), integrated with a custom-made sheath with 25mm outer diameter [15]. The sheath encases both the transducer and the source fibers. The inner surface of the sheath and the outer surface of the ultrasound transducer are covered with an aluminum material having a reflection coefficient of 85% at 750nm for high-intensity light output. The laser source was a tunable Ti: Sapphire laser (Symphotics TII, LS-2211) pumped by a Q-switched Nd:YAG laser (Symphotics TII, LS-2134). It delivered 20ns pulses at 15Hz repetition rate with 20mJ/pulse at the imaging wavelength of 750nm. The real-time image acquisition system for image processing and display was designed and implemented by our group [16,17].

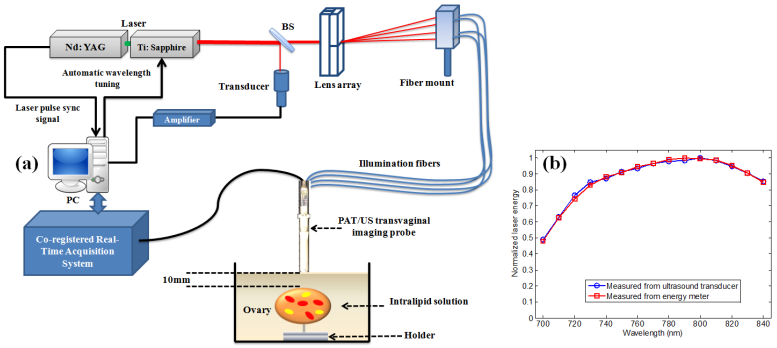

Fig. 1. (a) Experimental setup for ex vivo co-registered photoacoustic/ultrasound imaging. (b) Normalized laser output energy measured with single element ultrasound transducer and energy meter.

2.3 Laser energy monitoring

During the experiment, the laser output energy was monitored by a single element ultrasound transducer that receives small portion of the light from a beamsplitter as shown in Fig. 1(a). The wavelength of the laser was automatically tuned from 700nm to 840nm with 10nm step. To verify that the Radio frequency (RF) signal from the transducer monitor correlates well with the laser energy measured with the energy meter, the laser output energy measured at each wavelength using the transducer and energy meter was compared (Fig. 1(b)). The laser

#213817 - $15.00 USD Received 16 Jun 2014; revised 29 Jul 2014; accepted 11 Aug 2014; published 19 Aug 2014

source exhibits a drift in its output over time in addition to laser intensity fluctuations which occur more rapidly over very short periods of time. Consequently, the photoacoustic signal intensity generated during the imaging is affected by the drift and fluctuations. The single element transducer is able to accurately track and compensate the fluctuations and drift. The laser energy density on the tissue surface was ~20mJ/cm^2 at 750nm wavelength, which is below ANSI safety limit (24mJ/cm^2) [19]. The laser beam profile on the tissue surface was elliptical in shape with a semi-major and semi-minor axis of 0.35cm and 0.3cm respectively. The illumination area of the beam was calculated as an elliptical area.

2.4 In vivo and ex vivo studies

The animal protocol was approved by the institutional animal care and use committee of the University of Connecticut. *In vivo* photoacoustic/ultrasound imaging was performed on a sedated mouse under anesthesia by the inhalation of 1.5% isoflurane, and calibrated intralipid solution was used as a coupling medium in a framed plastic bag atop the mouse tumor. The co-registered sO_2/ultrasound image was obtained using PAT acquisitions at 14 wavelengths (710nm to 840nm with 10nm step) [16]. 5% of the laser output energy was split and directed to the single element transducer to monitor the variations in the laser intensity (Fig. 1(a)). This transducer was synchronized with the real time imager and laser source using a National Instrument data acquisition board (NI 5112). The signal output from the transducer was then used to compensate for the variations in the local fluence during the sO_2 measurement.

Human ovaries were obtained from patients undergoing prophylactic oophorectomy at the University of Connecticut Health Center (UCHC). These patients were at risk for ovarian cancer or they had ovarian mass or pelvic mass suggesting malignancy. This study was approved by the Institutional Review Boards of UCHC, and informed consent was obtained from all patients. Ovaries were kept in the 0.9% wt/vol NaCl solution and imaged within 24 hours after oophorectomy. During *ex vivo* imaging, human ovary was immersed in intralipid solution with μ_a of 0.04 cm^{-1} and μ'_s of 4cm^{-1}. Each ovary was mounted on a supporting frame made of a transparent thin optical fiber net and immersed inside a calibrated intralipid solution tank. The ovary was located ~10mm deep from the imaging probe base. In general, most ovaries are expected to be imaged *in vivo* at depth of ~8 to10mm which is the thickness of human vaginal muscle wall. This muscle wall, being the intervening structure between the imaging probe and the ovary, will absorb and scatter some of the light. The ovaries were imaged with an average of 32 laser pulses, 45dB US dynamic range and 15dB PAT dynamic range. After photoacoustic/ultrasound imaging, the ovaries were fixed in 10% formalin solution and returned to the Pathology Department for histological processing.

3. Results and discussion

The laser beam profilers at various distances from the lens array are shown in Fig. 2. The lens array could split the laser beam into four separate and equal spots if the laser light passed

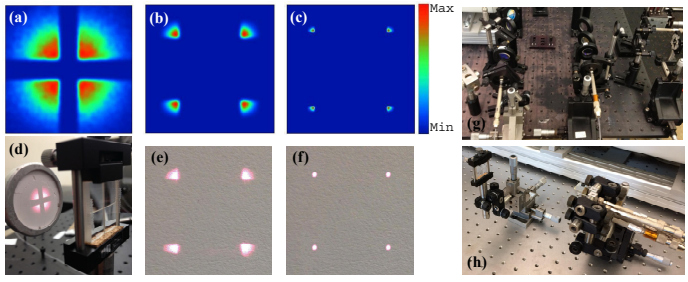

Fig. 2. (a) Simulated laser beam profile at 40mm away from the lens array, (b) 120mm away from the lens array, (c) 140mm away from the lens array. (d) Photograph of the designed lens array and experimental validation at ~40mm away from the lens array, (e) experimental validation at ~120mm, and (f) experimental validation at ~140mm. (g) Illumination setup before miniaturization, (h) after miniaturization.

#213817 - $15.00 USD Received 16 Jun 2014; revised 29 Jul 2014; accepted 11 Aug 2014; published 19 Aug 2014

through the array center. Figures 2(a), 2(b), and 2(c) demonstrate the simulated beam profiles at 40, 120, and 140mm away from the lens array. Figures 2(d), 2(e), and 2(f) show that the constructed lens array similarly divides the incident light into four equal beams that can be coupled to the optical fibers. This design makes our optical setup extremely compact. In addition, the design employs much fewer optical components and is thus much simpler and less expensive. Shown in Figs. 2(g) and 2(h) are the illumination setup before (setup size: 50 × 70cm) and after miniaturization (setup size: 10 × 20cm). Moreover, the lens array along with optical fibers deliver Gaussian beams to the tissue without any distortion as observed in Figs. 3(a) and 3(b). The beam profile was obtained after light propagation through the optical fiber. By using this miniaturized illumination setup, the signal-to-noise ratio (SNR) for imaging of polyethylene tubing filled with rat blood was 25dB, whereas the SNR for the same phantom image was 22.5dB when the setup in Fig. 2(g) was utilized. Therefore, this new design has demonstrated up to 2.5dB improvement in image quality. The SNR is defined as the mean of photoacoustic signals obtained from the phantom target divided by the background noise measured at the region with no light illumination.

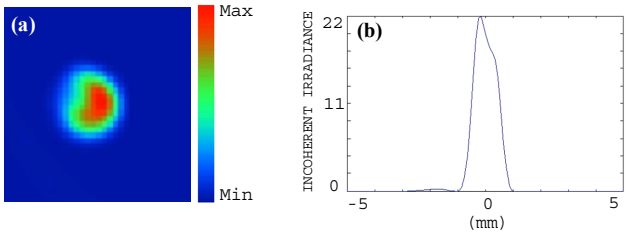

Fig. 3. (a) Simulated laser beam profile after propagating through the optical fiber. (b) The corresponding one-dimensional profile of the beam.

Shown in Figs. 4(a), 4(b), and 4(c) are three co-registered photoacoustic/ultrasound images of a mouse tumor and selected at wavelengths of 750, 800 and 840nm. The pulse-echo image is displayed in gray scale and the photoacoustic image in color scale. Figure 4(d) demonstrates the corresponding co-registered sO_2 image with the percentage of oxygen saturation of the blood hemoglobin within the tumor area. This image shows higher oxygenation at the edge of the tumor compared with the level in the tumor core. The skin surface in general has a higher absorption coefficient at lower wavelengths due to the higher deoxygenated hemoglobin content, and thus lower sO_2. This low sO_2 levels can be clearly seen in the sO_2 image shown in Fig. 4(d). The sO_2 image was produced using least square fitting technique to find an estimate of the oxygenated hemoglobin (HbO_2) and deoxygenated hemoglobin (Hb) concentrations for every pixel using the PAT measurements at 14 wavelengths (710-840nm with 10nm interval).

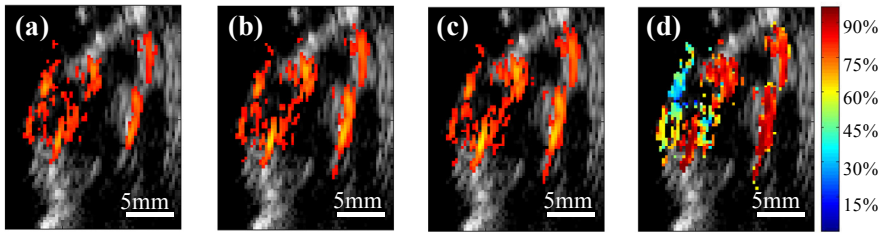

Fig. 4. *In vivo* co-registered photoacoustic/ultrasound images of the tumor area at wavelength of (a) 750nm, (b) 800nm, and (c) 840nm. (d) The co-registered ultrasound and oxygen saturation (sO_2) image obtained from PAT acquisitions at 14 different wavelengths.

To demonstrate the potential of our probe for ovarian cancer detection, human ovarian tissues were imaged *ex vivo*. Figure 5(a) shows an image example of an ovary from a 40-year-old high-risk patient. The ultrasound image reveals the presence of several antral follicles,

#213817 - $15.00 USD Received 16 Jun 2014; revised 29 Jul 2014; accepted 11 Aug 2014; published 19 Aug 2014

which are typical of normal premenopausal ovaries. Moreover, the photoacoustic image indicates that most of the light absorption takes place in the theca, which surrounds the antral follicle and is rich in vasculature [8]. The cause of the light absorption is the presence of blood in the theca, and the volume depends on the current stage of the development of the follicle. Histological evaluation by hematoxylin and eosin (H&E) staining of the sample reveals a benign premenopausal ovary as illustrated in Fig. 5(b), and the scattered microvessels around the follicles are observed in Fig. 5(c). A co-registered image of a malignant ovary from a 69-year-old postmenopausal woman is shown in Fig. 6(a). The ultrasound image shows homogeneous tissue pattern, however, high vascular areas at the surface compared with the surrounding tissue are observed in the photoacoustic image. Figure 6(b) that stained with H&E and marked by a white circle, reveals clusters of small vessels and malignant cancer cells in the ovary.

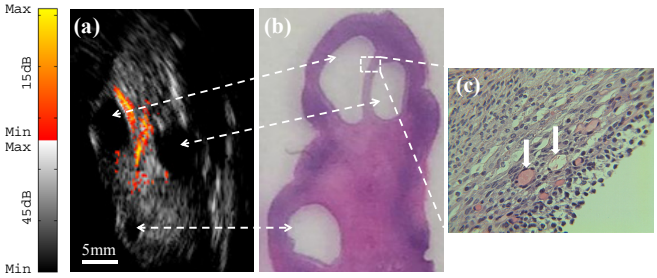

Fig. 5. (a) *Ex vivo* co-registered photoacoustic/ultrasound image of premenopausal ovary with benign tissue; (b) H&E staining of the corresponding area (× 1); (c) Reveals microvessels around the follicles (× 40) from the rectangular region indicated in (b).

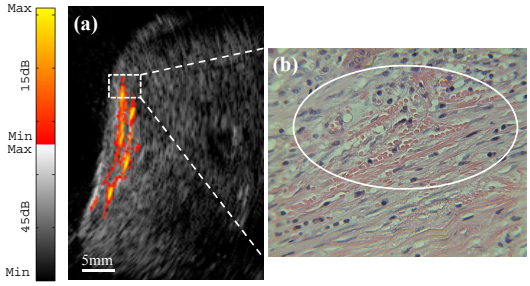

Fig. 6. (a) *Ex vivo* co-registered photoacoustic/ultrasound image of postmenopausal ovary with malignancy. (b) Reveals a cluster of microvessels (× 40) from the rectangular region indicated in (a).

4. Summary

A compact light delivery system for transvaginal co-registered photoacoustic/ultrasound imaging of ovarian tissue has been designed and implemented. The spatial and spectroscopic imaging capability of the co-registered imaging system has been demonstrated using *in vivo* mouse tumor model. Furthermore, *ex vivo* benign and malignant human ovarian tissues were imaged by the co-registered imaging system to visualize the blood vascular on the surface and inside, and that could be extremely valuable in assisting physicians for *in vivo* evaluation of ovarian tissue and early cancer detection.

Acknowledgments

Authors thank Feifei Zhou for helping with the mice experiments. Dr. Molly Brewer and Dr. Melinda Sanders are thanked for providing the ovaries and reviewing the pathology. This research is supported by the National Cancer Institute (NIH R01CA151570).

#213817 - $15.00 USD Received 16 Jun 2014; revised 29 Jul 2014; accepted 11 Aug 2014; published 19 Aug 2014